Human Molecular Genetics, 2008, Vol. 17, No. 24 **3929–3941**
doi:10.1093/hmg/ddn295
Advance Access published on September 18, 2008

Age-related retinal degeneration (*arrd2*) in a novel mouse model due to a nonsense mutation in the *Mdm1* gene

Bo Chang[1,†,¶], Md Nawajes A. Mandal[2,†,¶], Venkata R.M. Chavali[2,‡], Norman L. Hawes[1], Naheed W. Khan[2], Ronald E. Hurd[1], Richard S. Smith[1], Muriel L. Davisson[1], Laura Kopplin[3], Barbara E.K. Klein[4], Ronald Klein[4], Sudha K. Iyengar[3], John R. Heckenlively[2] and Radha Ayyagari[2,*,‡]

[1]The Jackson Laboratory, Bar Harbor, ME 04609, USA, [2]W.K. Kellogg Eye Center, The University of Michigan, 1000 Wall Street, Ann Arbor, MI 48105, USA, [3]Department of Epidemiology and Biostatistics, Case Western Reserve University, Cleveland, OH 44106, USA and [4]Department of Ophthalmology and Visual Sciences, University of Wisconsin-Madison, Madison, WI 53705, USA

Received July 2, 2008; Revised August 25, 2008; Accepted September 9, 2008

We observed that a naturally occurring mouse strain developed age-related retinal degeneration (*arrd2*). These mice had normal fundi, electroretinograms (ERGs) and retinal histology at 6 months of age; vessel attenuation, RPE atrophy and pigmentary abnormalities at 14 months, which progressed to complete loss of photoreceptors and extinguished ERG by 22 months. Genetic analysis revealed that the retinal degeneration in *arrd2* segregates in an autosomal recessive manner and the disease gene localizes to mouse chromosome 10. A positional candidate cloning approach detected a nonsense mutation in the mouse double minute-1 gene (*Mdm1*), which results in the truncation of the putative protein from 718 amino acids to 398. We have identified a novel transcript of the *Mdm1* gene, which is the predominant transcript in the retina. The *Mdm1* transcript is localized to the nuclear layers of neural retina. Expression of *Mdm1* in the retina increases steadily from post-natal day 30 to 1 year, and a high level of *Mdm1* are subsequently maintained. The *Mdm1* transcript was found to be significantly depleted in the retina of *arrd2* mice and the transcript was observed to degrade by nonsense-mediated decay. These results indicate that the depletion of the *Mdm1* transcript may underlie the mechanism leading to late-onset progressive retinal degeneration in *arrd2* mice. Analysis of a cohort of patients with age-related macular degeneration (AMD) wherein the susceptibility locus maps to chromosome 12q, a region bearing the human ortholog to *MDM1*, did not reveal association between human *MDM1* and AMD.

INTRODUCTION

Retinal degenerations are a group of disorders that cause irreversible loss of vision. Clinically, a wide variety of inherited retinal degenerations have been described both in animal models and humans (1). Genes involved in causing more than 140 human retinal degenerations have been identified (RetNet: http://www.sph.uth.tmc.edu/Retnet/). Orthologs of some of these genes were found to be associated with retinal degenerations in animal models. Mouse models with retinal degenerations have provided insight into the etiology of human retinal degenerations and molecular pathology of disease progression (1). Some of these animals develop late-onset retinal degeneration, but a majority of them show slow progression of the disease with a less severe phenotype and onset before the age of 6 months (2). Animal models

*To whom correspondence should be addressed. Tel: +1 8585349029; Fax: +1 8585348293; Email: rayyagari@ucsd.edu
†Present Address: Department of Ophthalmology, OUHSC, Oklahoma City, OK, USA.
‡Present Address: Jacobs Retina Center, Rm 206, Shiley Eye Center, University of California San Diego, 9415 Campus Point Drive, La Jolla, CA 92093-0946, USA.
¶The authors wish it to be known that, in their opinion, the first two authors should be regarded as joint First Authors.

with a shorter life span serve as valuable tools to study human diseases particularly conditions that manifest late in life (3).

Degeneration of the central part of retina, the macula, is observed in age-related macular degeneration (AMD) that affects 1 in 20 Americans of 65 years of age or older (4). AMD is a progressive and chronic degeneration that in its late stage may involve the photoreceptors, the underlying retinal pigmented epithelium (RPE), Bruch's membrane and possibly the choriocapillaries in the macular region of the eye. Clinical features of AMD include hypo- and hyper-pigmentation, deposition of drusen, loss of photoreceptors, RPE abnormality and formation of choroidal neovascularization membrane (5–7). Several genes associated with AMD have been reported (8–11) implicating perturbations in the complement pathway and other genes in susceptibility to disease. Despite these significant advances, much remains to be discovered about the biological mechanisms that lead to late-onset degeneration in AMD.

In this study, we describe the characterization of a novel and naturally occurring mouse model with autosomal recessive late-onset severe retinal degeneration, *arrd2*, primarily involving the neural retina. We mapped the disease gene to mouse chromosome 10 and identified a nonsense mutation in a novel retina expressed transcript of the *Mus musculus* double minute 1 (*Mdm1*) gene. This gene was first identified in transformed mouse 3T3 cells along with the oncoprotein *Mdm2*. Both *Mdm1* and *Mdm2* are localized to mouse chromosome 10. Although *Mdm2* is a well-studied gene, very little is known about *Mdm1* (12,13). In this article, we present the characterization of a novel retina-expressed transcript of the *Mdm1*, expression profile of different transcripts of this gene, localization of its expression in the retina, molecular pathology and potential effect of the *Mdm1* nonsense mutation leading to degeneration of retina in *arrd2* mice. We also examine the relation of the human *MDM1* to AMD.

RESULTS

Phenotype of *arrd2* mice retina

Fundus examination of the homozygous *arrd2* mice revealed no abnormality at 6 months of age (Fig. 1A, i and iii). The retinas of these mice at 14 months showed significant retinal hypo- and hyper-pigmentation (Fig. 1A, ii and iv). Signs of retinal degeneration such as vessel attenuation, alterations in the RPE and the presence of retinal dots were noted at 14 months of age. Electroretinogram (ERG) responses of *arrd2* mice were found to be normal at 6 months (data not sown). The dark-adapted and light-adapted ERG response showed progressive amplitude loss from 8 to 16 months (Fig. 1B). The rod response is minimal at 16 months with some sparing of the cone responses (Fig. 1B). By 22 months, both rod and cone ERG responses were undetectable (data not shown). Histological analysis of the retina of *arrd2* mice showed slight reduction in the length of the outer segment (OS) and thickness of outer nuclear layer (ONL) by 9 months (Fig. 1C) and the length of OS and the thickness of ONL decreased progressively with age. By age 19 months, the OS and ONL were nearly absent in *arrd2* homozygous mice (Fig. 1C). The RPE cells at this age were found to be atrophic and hypo-pigmented.

Ultrastructural analysis by transmission electron microscopy (TEM) indicated minimal changes in the retinas of *arrd2* mice at 4 months. At this age, normal retinal architecture is maintained for the most part. In a few areas, minimal breakdown of OS architecture was observed suggesting increased numbers of phagosomes in the retinal pigment epithelium (Fig. 2A, black arrow). Inner segments, external limiting membrane and ONL are normal except for an occasional swollen synaptic terminal in the outer plexiform layer (Fig. 2B). The synaptic terminals have dense cytoplasm and large round mitochondria with complex, well-organized cristae (Fig. 2C). By 9 months of age, there is a prominent swelling and lucency of many synaptic terminals, some of which appear necrotic (Fig. 2D). In addition, swollen and necrotic cells are frequent in the inner nuclear layer adjacent to the outer plexiform layer, which is thinner than normal (Fig. 2E). The mitochondria of the synaptic terminals are swollen and demonstrate disorganization of the cristae (Fig. 2F, white arrows) and occasional malformation of the synaptic complexes (Fig. 2F, black arrow). The changes observed in the plexiform layers as early as 4 months indicate the possibility of early changes in the synaptic layers (Fig. 2C). OS fragmentation is a prominent feature (Fig. 2G, arrows) and there is a moderate increase in phagosome number in the retinal pigment epithelium. In addition, most of the apical processes of the retinal pigment epithelium are absent (Fig. 2H, arrow). Furthermore, the presence of lipofuscin-like granules was observed in the RPE (Fig. 2H, arrow-heads). Additional studies are needed to confirm lipofuscin accumulation in these mice.

Fundus examination of heterozygous *arrd2* mice did not reveal abnormality even at older ages. The dark-adapted and light-adapted ERG response of *arrd2/wt* mice is normal at age 12 and 22 months (data not shown).

Genetic analysis

Genetic analysis showed that the late-onset retinal degeneration in *arrd2* mice is an autosomal recessive trait. By linkage analysis of inter-crossed mice, we mapped the causative gene defect in *arrd2* to mouse chromosome 10 in the genomic region flanked by D10Mit179 (116.7 M) and D10Mit267 (119.1 M) (Fig. 3A and B). Among the 35 genes localized to this interval, 9 were found to be expressed in retina. Sequence analysis of retina-expressed candidate genes-like *Carboxypeptidase M* (*Cpm*), *Nucleoporin107* (*Nup107*), *Transformed mouse 3T3 double minute protein2 (Mdm2)*, *Solute carrier family 35 member E3* (*Slc35e3*), *Glutamate receptor interacting protein 1* (*Grip1*), *Kinesin family member C5C* (*Kifc5c*), *Interlukin 10-relative T cell-derived protein* (*Iltifb*), *Interferon gama* (*Infg*) revealed no mutational changes.

Furthermore, a single base C to T nonsense substitution (CGA to TGA) at position 1195 (Arg 399 stop) in exon VIII of a novel transcript of the *Mdm1* gene was observed in the homozygous state (GenBank ID: 1064299). The *Mdm1* nonsense mutation is predicted to result in truncation of the protein by 320 amino acids due to a premature termination at codon 399 (Fig. 3C). This single base substitution was confirmed by sequencing additional *arrd2* homozygous mice and

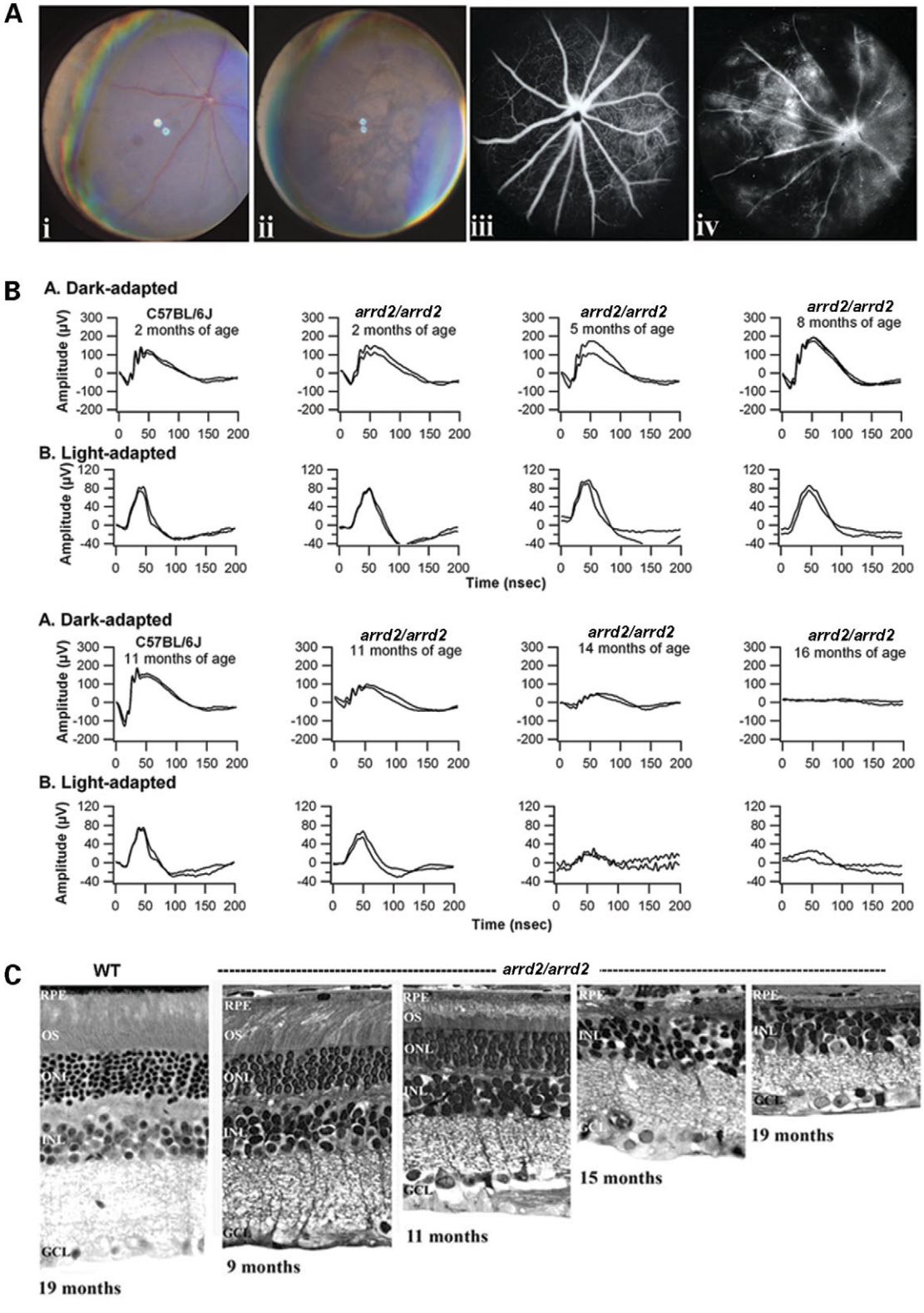

Figure 1. Retinal phenotype of *arrd2/arrd2* mouse. (**A**) Fundus photographs (A, i and ii) and fluorescein angiograms (A, iii and iv) of *arrd2/arrd2* mice at age 6 months with a normal fundus (A, i and iii) and at 14 months with retinal degeneration (A, ii and iv) demonstrating areas of hypo- and hyper-pigmentation and attenuated vessels. (**B**) Representative samples of rod- and cone-mediated ERGs in *arrd2/arrd2* mice at various ages. ERG b-wave amplitude at 198 μV (rod) and 87 μV (cone) was normal until about 8 months of age. B-wave amplitude progressively decreased with age until 16 months of age, and was non-recordable at 22 months (data not shown). (**C**) Representative samples of histological sections of retina in *arrd2/arrd2* mice. There was slight reduction in the length of OS and the thickness of ONL at 9 months. However, the length of the OS and thickness of ONL were progressively decreased with age at 11 and 15 months. By 19 months, the OS and ONL were nearly absent in *arrd2/arrd2* mice. GCL, ganglion cell layer; INL, inner nuclear layer; ONL, outer nuclear layer; OS, outer segment; RPE, retinal pigment epithelial layer.

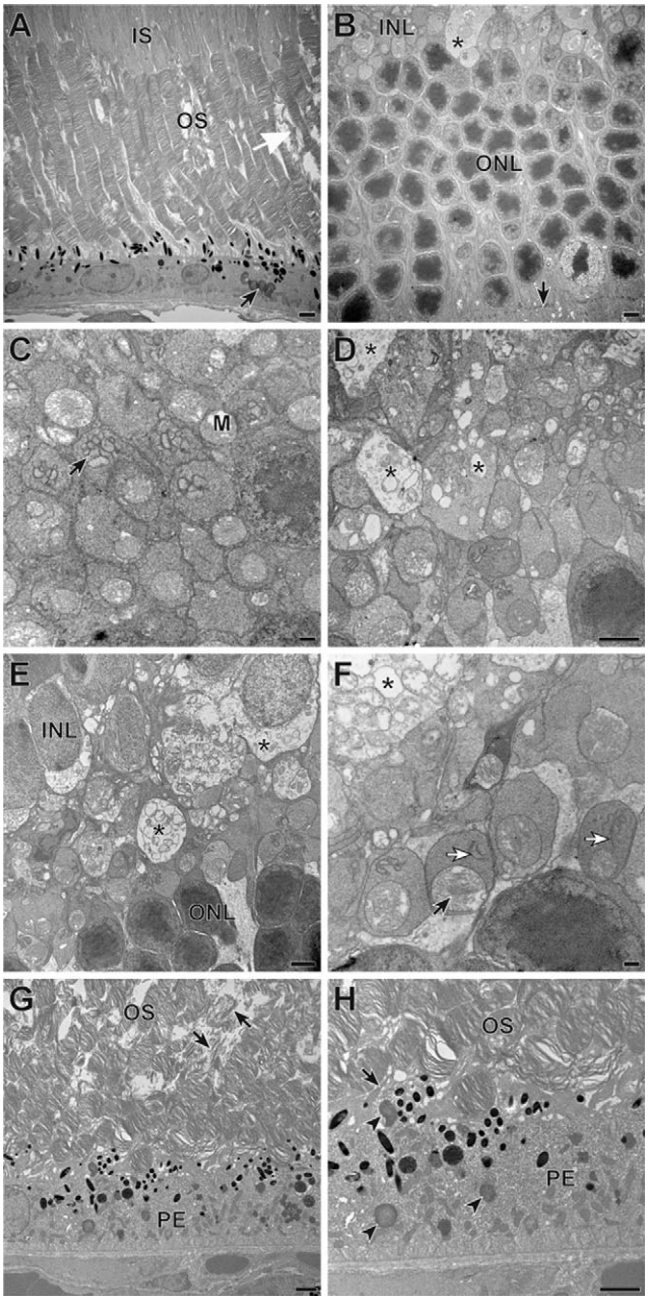

Figure 2. Electron micrographs depicting the outer retina of the *arrd2/arrd2* mouse. (**A**) *arrd2/arrd2* mouse at 4 months of age. The inner segments (IS) are normal. Most of the OS are normal, but in places there is mild disorganization (white arrow). This early OS degeneration may be the reason for the large clumps of photoreceptor debris in the retinal pigment epithelium (black arrow). (**B**) *arrd2/arrd2* mouse at 4 months of age. ONL morphology is normal and a well-developed external limiting membrane is present (black arrow). The outer plexiform layer is also normal except for a more lucent and swollen synaptic complex (*) that may be a sign of early damage. The arrow is pointing to a well-developed external limiting membrane. (**C**) *arrd2/arrd2* mouse at 4 months of age. The inner plexiform layer contains many complex synaptic terminals characterized by dense cytoplasm and large mitochondria (M) that have dense, well-organized cristae. (**D**) *arrd2/arrd2* mouse at 9 months of age. Many of the synaptic terminals are swollen (asterisks) and extreme cytoplasmic lucency in some suggests necrosis. (**E**) *arrd2/arrd2* mouse at 9 months of age. The outer plexiform layer is much thinner than normal, as indicated by the nuclei of the inner (INL) and outer (ONL) layers. Both synaptic terminals and cells of the inner nuclear layer are swollen and necrotic (*). (**F**) *arrd2/arrd2* mouse at 9 months of age. Mitochondria of the synaptic terminals are swollen with irregular cristae (black arrow). In some terminals, the synaptic complex is incompletely formed (white arrows). A portion of a necrotic cell from the inner nuclear layer (*) shows vacuolation and mitochondrial swelling. (**G**) *arrd2/arrd2* mouse at 9 months of age. The OS are fragmented (arrows). The retinal pigment epithelium (PE) is grossly normal. (**H**) At higher power, phagosomes (arrowheads) are abundant in the retinal pigment epithelium. The normally abundant apical processes of the pigment epithelium are rarely seen (arrow) Bar = 2μM (A, B, D, E, G and H); Bar = 500 nm (C and F).

this change was not detected in C57BL/6J, 129 Sv/J, CAST/EiJ and six additional wild strains of mice available at Jackson laboratories.

Characterization of the mouse *Mdm1* gene

The mouse *Mdm1* gene is known to have at least two transcripts, a longer transcript (LT) containing 14 exons (GI: 27229284) (Fig. 4A–I) and a shorter transcript (ST) (Fig. 4A, ii) containing only the first four exons (GI: 6754669). We observed a novel transcript in the retina by direct sequencing of mouse retinal cDNA, which is similar to the previously reported LT except for having an additional exon (total 15 exons) (GI: 1064299). The supplementary exon contains a 30 bp in-frame additional sequence (exon VIIa) and is located between exons VII and VIII. We refer to this transcript as the retinal transcript (RT) (Fig. 4A, iii). The *Mdm1* RT consists of an ORF of 718 amino acids and could encode a protein of nearly 80.7 kDa, the LT consists of an ORF of 708 amino acids and could encode a protein of nearly 79.6 kDa, and the ST consists of an ORF of 222 amino acids and could encode a protein of nearly 25.1 kDa. We also identified a variant of the RT which lacks exon IV (Fig. 4A, iv) (GI: 1064301). This confirms the existence of multiple *Mdm1* transcripts (12,13). As the *arrd2* mutation is in exon VIII, the LT and the RT will be affected by this mutation, and the short transcript (ST) that contains only four exons will not be affected.

Distribution of the LT and RT was tested by PCR and restriction digestion of these transcripts with restriction enzymes, *Nla III* and *Sex-A1* which specifically cut the RT and the LT without exon VIIa, respectively. Mouse tissue cDNAs were amplified with primers encompassing exon VI to exon IX and subjected to restriction digestion with the above enzymes. The retina expresses only the LT containing the novel additional exon, the RT (Fig. 4B, lanes: 10–12). Brain, lungs, anterior eye segments, and posterior eye segments (choroid-sclera, PS) express only the RT (Fig. 4B, lanes: 1–3, 4–6, 7–9, 13–15, respectively). The kidney, skeletal muscle, testis and uterine tissues express both RT and LT (Fig. 4B, lanes: 16–18, 19–21, 22–24, and 25–27, respectively). This analysis indicates that the novel transcript, RT, is expressed in several tissues including the retina. Sequence-based homology search revealed that this 30 bp region is also present in the human *MDM1* transcript. The significance of this 30 bp additional exon is not known. Blast search did not reveal any significant homology with any other known nucleotide or protein sequences in the databases (except *Mdm1* orthologs) indicating that this is a novel transcript.

We further studied the expression of different *Mdm1* transcripts in mouse tissue in order to understand the potential

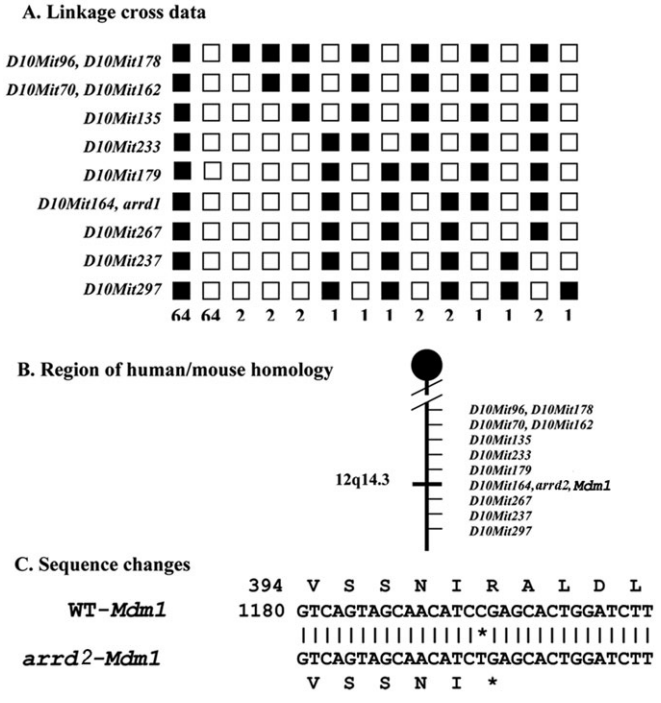

Figure 3. *Mdm1* mutation in *arrd2*. (**A**) Linkage cross-data: 73 inter-cross progeny from the (*arrd2*/C57BL/6J)F1 × (*arrd2*/C57BL/6J)F1 was phenotyped for histological phenotype and genotyped for the indicated microsatellite markers. Black boxes represent haplotypes for *arrd2*-derived alleles and white boxes represent haplotypes for C57BL/6J-derived alleles. The number of the corresponding haplotype is indicated below each column of squares. The order of marker loci was determined by minimizing the number of crossovers. The *arrd2* locus was inferred from the histological phenotype of mice showing recombinations. (**B**) Genetic map of mouse chromosome 10 showing the *arrd2* critical region, which is syntenic to human chromosome 12q14.3. (**C**) The nucleotide sequences around the single base substitution at position 1173 (C to T) in exon 9 are shown for the wild-type allele and the *arrd2* allele of the *Mdm1* gene. A novel mutation changes codon 399 CGA to A STOP CODON TGA (amino acid change: Arg399Ter) in the *Mdm1* gene in *arrd2/arrd2* mice. WT, wild type.

mechanism underlying retinal degeneration due to the nonsense mutation in the *Mdm1* gene. Using primers specific to the *Mdm1* RT, LT and short transcript (ST), the level of expression of each transcript was determined in different mouse tissues by quantitative RT–PCR (qRT–PCR). Among all the tissues tested, the highest level of expression of the RT was detected in the retina (Fig. 4C, top panel). Significant level of expression of this transcript was also detected in the testis, whereas low level of expression is observed in other tissues, including iris-ciliary body, kidney, skeletal muscle, heart and brain (Fig. 4C, top panel). The previously reported ST of the *Mdm1* gene showed significantly high level of expression in testis and very low level of expression in several tissues, including retina (Fig. 4C, middle panel). The previously known long transcript (LT) of the *Mdm1* gene was also found to be expressed at very high levels in testis (Fig. 4C, bottom panel). Earlier we observed that this LT was not present in brain and eye tissues, including the retina (Fig. 4B). Minimal levels of expression of LT were observed in kidney, skeletal muscle and uterine tissues by qRT–PCR.

Similar to several other retinal genes, the highest levels of *Mdm1* expression are observed in testis in addition to retina (14). Although the RT is the predominant transcript in the retina, low levels of *Mdm1* ST were also observed. Expression of *Mdm1* transcripts in other tissues tested was very low to insignificant compared to their levels in the retina and testis.

Retinal expression and location of *Mdm1* transcripts

We studied the expression profile of *Mdm1* in control (C57BL/6J) mice retina during post-natal development and aging. In developing eyes of normal mice, expression of this gene was detected from post-natal day 1 (data not shown). In the retina, a gradual increase in the expression of *Mdm1* transcripts, RT and ST, was observed from 1 to 6 months of age (Fig. 5A). After 6 months, the expression level remained unchanged up to 20 months, the highest age point we have tested, indicating that the presence of high level of *Mdm1* expression may be important for adult retinal tissue.

By *in situ* hybridization, expression of the *Mdm1* gene (the RT) in wild-type albino mouse retinal sections was detected in all the nuclear layers of the neural retina: the ONL, inner nuclear layer and also the ganglion cell layer (Fig. 5B, arrows). Presence of *Mdm1* was not detected in the RPE.

Molecular characterization of *arrd2* retina

To gain insight into the pathology of degeneration, we studied the expression profile of different marker genes in *arrd2* and age-matched wild-type control mice (C57BL/6J) retina at three time points: 5, 12 and 18 months of age. In Figure 6, we presented the expression profile of selected marker genes in *arrd2* retina in comparison to controls, by taking the expression values of these genes in age-matched controls as 100%. At 5 months, the expression of rod OS proteins, rhodopsin and RDS, was not significantly different from wild-type retina, but reduced to ∼40% by 12 months and to insignificant levels by 18 months (Fig. 6A). Interestingly, rod inner segment protein arrestin (*Sag*) expression was higher (150–180% of wild-type) in *arrd2* retina at 5 and 12 months (Fig. 6A). The cone photoreceptor marker, short-wave length cone opsin (*Opn1-sw*) was slightly reduced (70%) at 5 months and subsequently remained unaltered up to 12 months (Fig. 6B). Medium-wavelength cone opsin (*Opn1-mw*) was reduced to ∼45% at 5 months and gradually reduced to ∼25 and ∼5% by 12 and 18 months, respectively (Fig. 6B). Furthermore, the expression of cone inner segment protein cone transducin (*Gnat2*) showed gradual reduction and remained at ∼40% of the levels compared to controls at 18 months when the levels of most of the OS proteins are insignificant in *arrd2* mice retina. Expression of *Elongation of very long chain fatty acid 4* (*Elovl4*), which is an inner segment protein of both rod and cone photoreceptors, is reduced to ∼60% by 12 months and to ∼20% by 18 months (Fig. 6B). In summary, the expression profile of retinal cell marker genes suggests loss of both rod and cone photoreceptors cells between 5 and 12 months and sparing of a few cones at 18 months. The degeneration of cones appears to be slower than rods and these observations are consistent with the observations made by histology and ERG analysis (Fig. 1).

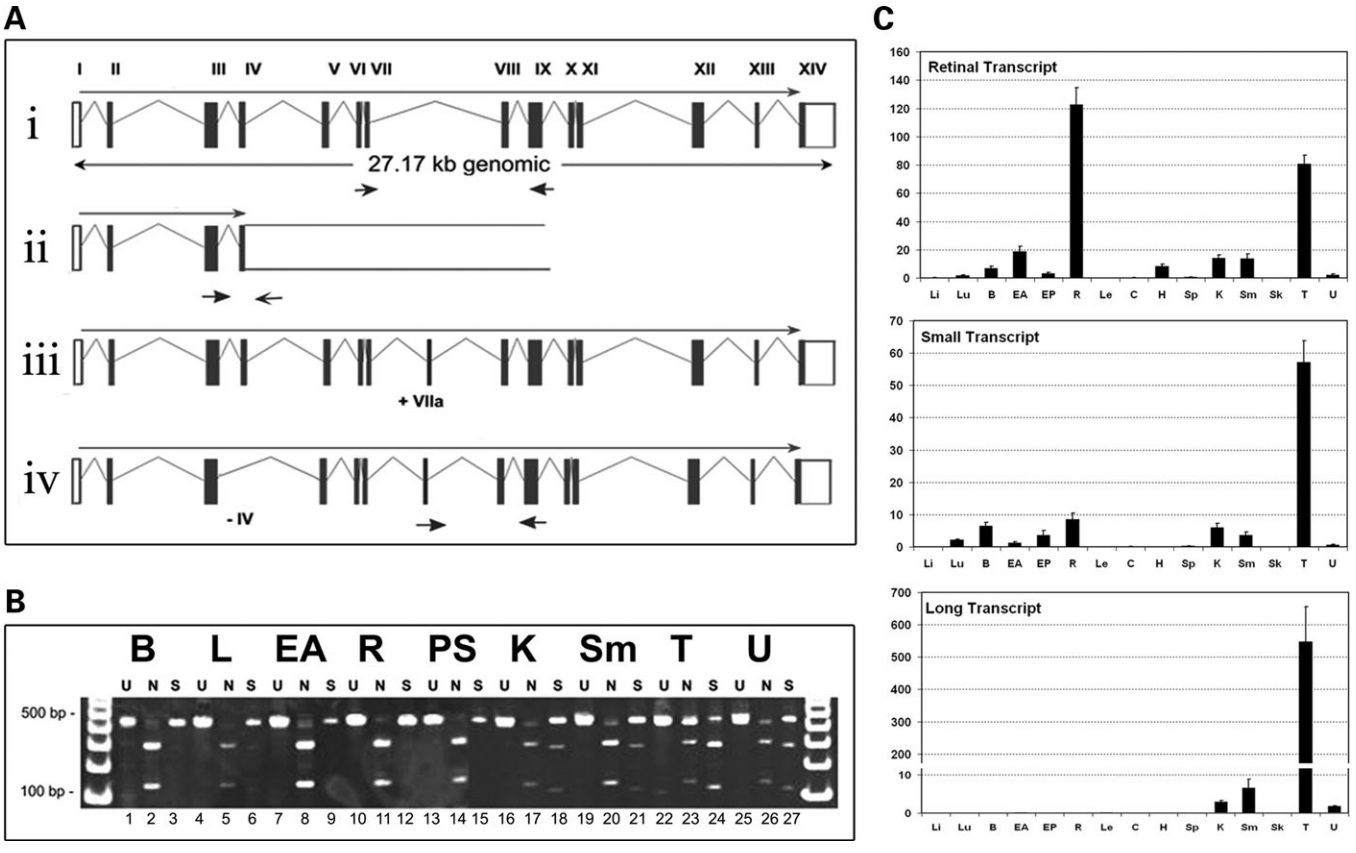

Figure 4. Structure and distribution of Mdm1 transcripts. (**A-i**) Schematic drawing of *Mdm1* LT which is previously reported and having 14 exons (I–XIV). The length of the introns and exons is not in scale. (A-ii) Mdm1 ST with four exons which have been reported earlier (I –IV). (A-iii) Mdm1 novel transcript, RT which has 15 exons including the novel 30 bp exon (VIIa). (A-iv) A variant of Mdm1 RT which lacks exon IV. (**B**) Tissue specific distribution of *Mdm1* LTs. *Mdm1* fragments spanning from exon VI to exon IX are amplified from cDNA of mouse brain (B), lungs (L), eye anterior (EA, include iris, ciliary body and cornea), retina (R), posterior segment (PS, includes RPE, choroid and sclera), kidney (K), skeletal muscle (Sm), testis (T) and uterus (U), and subjected to digestion with *Nla* III and *Sex* AI restriction enzymes which specifically cut amplified sequences of the RT and LT, respectively. Each sample was loaded in three lanes: 'U' represents un-cut, 'N' represents cut by *Nla* III and 'S' represents cut by *Sex* AI. Brain, lungs, eye anterior, retina, posterior segment tissues express only the RT but the kidney, skeletal muscle, testis and uterus tissue express both transcripts. (**C**) Quantitative expression of different *Mdm1* transcripts in adult mouse tissues. Quantitative expression of different *Mdm1* transcripts are measured by real-time PCR and presented in a relative scale which is equivalent to 'per 10,000 of *β-Actin* expression'. The expression values are calculated from at least three independent samples each with three replication PCRs. Top panel shows the expression of the RT; middle panel shows the expression of the ST and the bottom panel represents the expression of the LT.

Expression of glial fibrillary acidic protein (*Gfap*), a common retinal stress response marker, was found to be more than 20-fold higher (>2000% of control) even at 5 months (Fig. 6C). It gradually increased to >20 000% (200-fold) by 18 months (Fig. 6C). Expression of oxidative stress or redox-mediated stress markers *Heme oxygenase 1* (*Ho-1*) and *Ceruloplasmin* (*Cp*) was not altered up to 12 months. Subsequently, expression of these genes increased significantly at 18 months, when the retina is appreciably degenerated (Fig. 6C). The apoptosis marker *Caspase 3* (*Casp3*) and angiogenesis marker *Vascular endothelial growth factor* (*Vegf*) also showed expression pattern similar to *Ho-1* and *Cp* (Fig. 6D).

Fate of *Mdm1* transcripts in *arrd2* retina

By qRT–PCR analysis of *arrd2* mouse retina, the level of *Mdm1* RT was found to be reduced to ∼40% of wild-type (C57BL/6J) retina by 5 months (Fig. 7A). By 12 months, the level of RT in the retina of *arrd2* mice was <20% of the levels observed in C57BL/6J retina (Fig. 7A). The level of expression of RT was further reduced to ∼5% of the levels observed in C57BL/6J retina by 18 months (Fig. 7A). On the other hand, the *Mdm1* small transcript (ST) showed elevated expression at 5 months: >250% of C57BL/6J retina (Fig. 7A). Subsequently, it was also reduced to ∼25 and ∼20% of the wild-type by 12 and 18 months of age, respectively (Fig. 7A). Significant reduction in the quantity of RT in *arrd2* retina before the onset of retinal degeneration suggests degradation or specific down regulation of the mutant transcript.

To further assess the fate of *Mdm1* RT, we analyzed *arrd2* retina and testis samples at 6 months by northern blot analysis using a probe that recognizes *Mdm1* RT and LT. The RNA samples isolated from C57BL/6J were used as controls for comparison. A strong ∼3.0 kb band representing *Mdm1* transcript was observed in the RNA isolated from C57 retina and testis (Fig. 7B; lanes 3 and 7). The bands corresponding to *Mdm1* LT or RT detected in *arrd2* mice retina and testis are very faint and almost insignificant in comparison to the

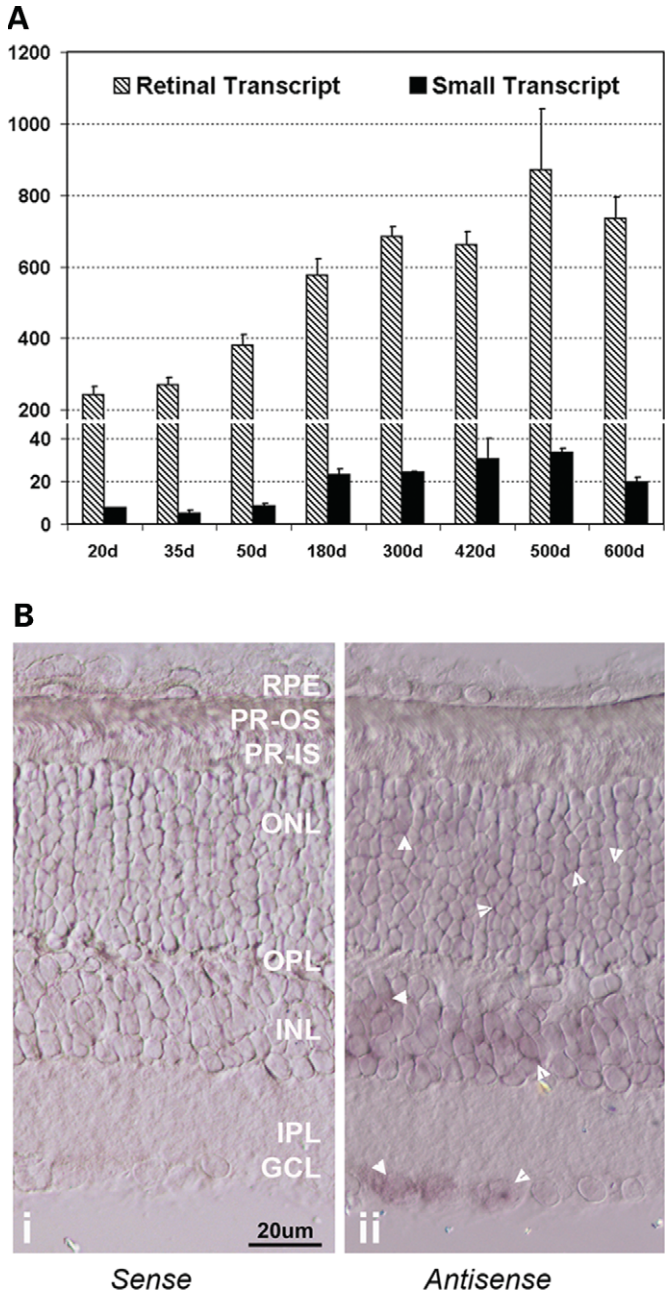

Figure 5. Expression of Mdm1 with age and location in the retina. (**A**) Quantitative expression of retina-expressing *Mdm1* transcripts (RT and ST) in mouse retina with age (20 to 600 days). Expression values are calculated from three independent samples and presented in a scale which is equivalent to 'per 1,000 of *Hgprt* expression'. (**B**) Localization of the *Mdm1* RTs in the albino mouse retina by ISH. *Mdm1* location is marked by the arrow-heads in the retinal section hybridized with antisense probe (B, ii). No specific labeling is detected in the section hybridized with the sense probe which served as a negative control (B, i). RPE, retinal pigmented epithelium; PR-OS, photoreceptor outer segment; PR-IS, photoreceptor inner segment; ONL, outer nuclear layer; OPL, outer plexiform layer; INL, inner nuclear layer; IPL, inner plexiform layer, GCL, ganglion cell layer.

intensity of these bands in retina and testis from age-matched control animals (Fig. 7B; lanes 4 and 8). A set of doublet bands were detected in the testis (Fig. 7B; lane 7). Both RT and LT are expressed in testis (Fig. 4). Therefore, the doublet bands detected by northern blot analysis in the C57BL/6J testis are likely to represent these two transcripts of the *Mdm1* gene. No significant expression is detected in kidney (Fig. 7B; lanes 1 and 2) and brain (Fig. 7B; lanes 5 and 6) tissues. The top and bottom panels of the Figure 7B showed the RNA quality and equal loading controls.

In agreement with the above observations, no significant labeling of *Mdm1* was detected in *arrd2* mouse retina by *in situ* hybridization at 3 months and at 10 months (data not shown). The mutation in the *Mdm1* gene in *arrd2* mice is a nonsense mutation in exon VIII which is 960 bp upstream of the original stop codon. Therefore, it is likely that this transcript is undergoing nonsense-mediated decay (NMD) in *arrd2* mice.

Assay for nonsense-mediated decay of *Mdm1* transcripts

To address the hypothesis that the reduction of the *Mdm1* transcript in the *arrd2* mouse retina is through NMD, we carried out NMD assay using retinal explants in culture and inhibiting translation with cycloheximide. When a nonsense mutation is detected by the translational machinery, through cellular proofreading, the nonsense mutation containing transcripts are degraded. Therefore, if the translation process in the cell is blocked, all transcripts get accumulated including the mRNA carrying the nonsense mutation.

Significant accumulation ($\sim$9-fold, $P = 0.004$) of the *Mdm1* RT was detected by qRT–PCR when the translation is blocked by cycloheximide for 4 h in 2-month-old *arrd2* mice retina (Fig. 8A; aR = *arrd2* retina). These accumulated transcripts were degraded to near zero levels within 2 h of withdrawal of the cycloheximide (Fig. 8A). In the control C57BL/6J retina, cycloheximide treatment increased the quantity of *Mdm1* transcript (not significantly) which returned back to normal level when the drug was withdrawn (Fig. 8A; CR = C57 retina). Similar results were observed when testis tissue of both the *arrd2* and control mice was subjected to NMD assay (Fig. 8B; aT = *arrd2* testis and CT = C57 testis). As an internal control, levels of *β-Actin* were tested in the *arrd2* mouse retinal and testis samples. Slight accumulation ($\sim$1.5-fold) of the *β-Actin* transcript was observed after 4 h of cycloheximide treatment in retinal samples, and after withdrawal of the drug the levels of *β-Actin* transcript returned to normal, but not to the near zero levels as observed for *Mdm1* transcript (Fig. 8C). No change was observed in the levels of this gene in testis tissues (Fig. 8C). We also tested the level of the ST in *arrd2* mice. It also showed slight accumulation with the treatment, but was significantly reduced after the removal of cycloheximide (Fig. 8D). These observations suggest that the stop codon mutation in the *Mdm1* gene results in degradation of the RT through NMD.

Evaluation of the association of *MDM1* gene with age-related macular degeneration in patients

To investigate the contribution of *MDM1* to AMD risk in humans, an association analysis was conducted in the 'Family Age Related Maculopathy Study (FARMS)' cohort, a Caucasian family-based study population in which an AMD locus was mapped to a region on chromosome 12 that

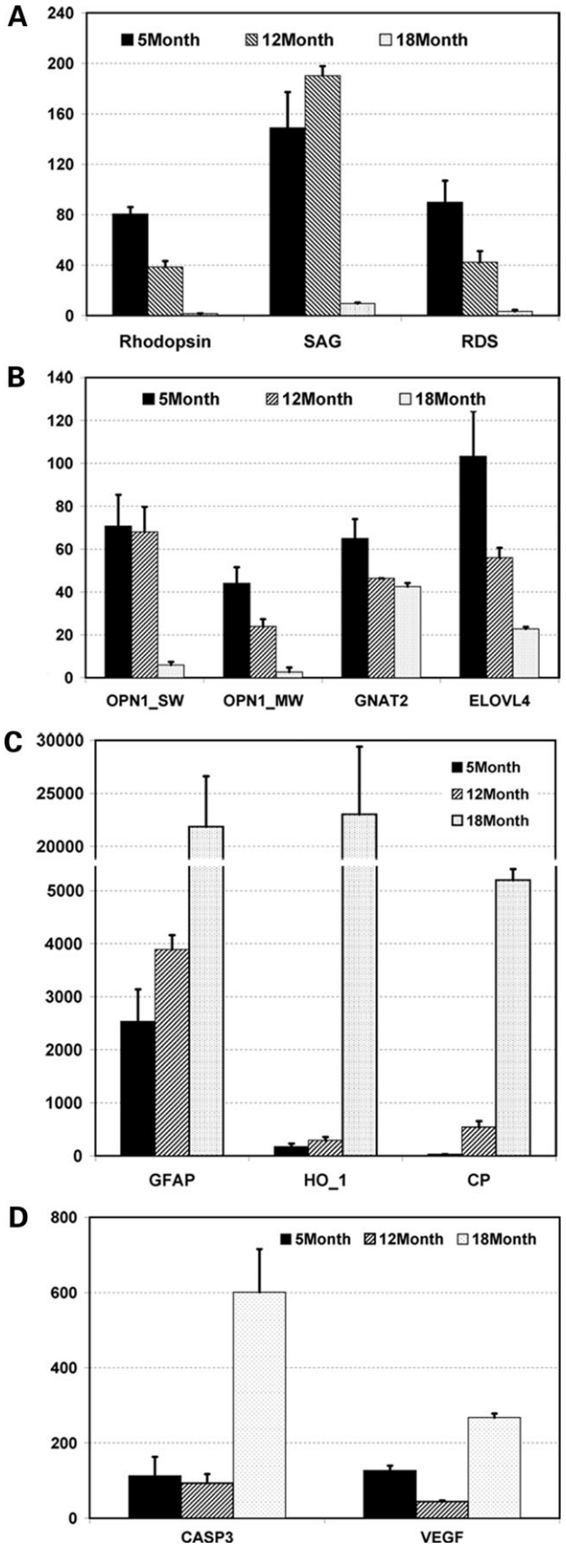

is syntenic to the region on mouse chromosome 10 harboring *Mdm1*. The human linkage peak on chromosome 12q is broad, spanning almost 36 cM and harboring 636 genes, 179 having known retinal expression according to BioMart and the GNF expression database. Three SNPs were chosen for analysis based on their predicted ability to represent the linkage disequilibrium (LD) structure at the *MDM1* locus. In addition, two of these variants result in missense mutations within the gene. Testing was completed using a variance component family-based association model that included family and sibling effects. None of the three SNPs displayed significant associations with AMD severity. rs962976 and rs2306392, the missense variants, were not statistically significant under any model tested. rs973328, a variant slightly 3′ to *MDM1*, demonstrated the most significant finding of association with AMD severity of the tested SNPs ($P = 0.08$, dominant model).

Database of genome wide association studies (*dbGaP*) was consulted to see if *MDM1* showed any significant findings in a sample of participants in the Age-Related Eye Disease Study (AREDS) cohort. The three SNPs examined in the FARMS cohort were also present in the AREDS analysis and were not reported to be significantly associated with AMD. In addition, the AREDS study reported non-significant findings of association between another six SNPs within *MDM1* and AMD. Thus, we conclude that the *Mdm1* locus is not the AMD locus on human chromosome 12.

DISCUSSION

We identified a naturally occurring mouse model with age-related progressive retinal degeneration (*arrd2*). These mice showed subnormal rod and cone ERGs at the age of 6 months progressing to undetectable ERG response by 22 months; slight decrease in photoreceptor nuclei at 9 months, to significant loss of photoreceptor layer by 20 months. We have mapped the disease locus to the mouse chromosome 10 and detected a nonsense mutation in the *mouse double minute 1* (*Mdm1*) gene that is likely to result in NMD of the transcript. Our studies indicate that the late-onset progressive retinal degeneration observed in these mice is likely to be due to the loss of functional MDM1 in the retina of *arrd2* mice.

The expression profile of photoreceptor-specific genes, electrophysiological responses and morphology of retina in *arrd2* mice indicated late-onset progressive photoreceptor degeneration with severe degeneration of both rods and cones. Although the age of onset is late, the rate of degeneration is much faster after 8 months with cone degeneration slower

Figure 6. Expression of marker genes in *arrd2* retina with age. Expression level of different retinal photoreceptor marker genes and stress-related genes is measured by quantitative real-time PCR at three different ages and the expression values are normalized against the house keeping gene (*Hgprt1*) and presented as percentage of the expression in wild-type (control) retina (C57BL/6J) at the same age. In all the figures, the arbitrary expression value for all the genes in control retina is 100. (**A**) Expression of Rod photoreceptor genes: *Rhodopsin*, Arrestin (*Sag*) and *Rds*. (**B**) Expression of Cone photoreceptor genes and *Elovl4*: Cone opsin short-wave (*Opn1-sw*), Cone opsin medium-wave (*Opn1-mw*), Cone transducin (*Gnat2*). (**C**) Expression of retinal stress-related gene *Gfap*, *Heme oxygenase-1* and *Ceruloplasmin*. (**D**) Expression of *Caspase 3* and *Vegf*.

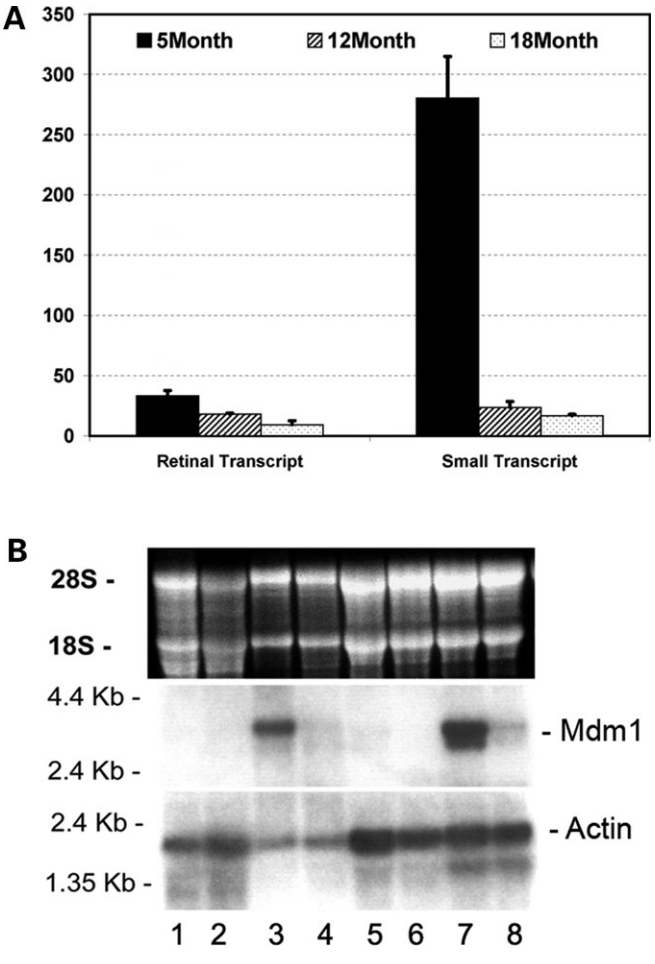

Figure 7. Expression of *Mdm1* transcripts in *arrd2* retina. (**A**) Expression level of *Mdm1* RT and ST is measured by quantitative real-time PCR at three different ages and the expression values are presented as percentage of the expression in wild-type retina (C57BL/6J) at the same age. (**B**) Detection of *Mdm1* RT by northern blotting. Equal quantity of total RNA extracted from different tissues of C57BL/6J and *arrd2* mice were run side by side on an agarose gel, blotted onto nylon membrane and probed with radio-labeled *Mdm1*fragment that recognizes the LTs. Lane 1, C57BL/6J kidney; lane 2, *arrd2* kidney; lane 3, C57BL/6J retina; lane 4, *arrd2* retina; lane 5, C57BL/6J brain; lane 6, *arrd2* brain; lane 7, C57BL/6J testis; lane 8, *arrd2* testis. Top panel is an image of the RNA gel showing 28S and 18S rRNA bands and the bottom panel shows the same blot probed with *β-Actin*, both of which indicate the equal loading of the *arrd2* and C57BL/6J samples.

than the rod degeneration. The phenotype of these mice with attenuation of retinal vessels, ERG abnormalities resembles late-onset, progressive rod-cone degeneration in humans. A large number of genes that cause retinal dystrophy in mice are also associated with retinal conditions in humans (15) and analysis of patients with clinical features similar to the phenotype observed in these mice may reveal the involvement of this gene in causing human retinal degeneration.

The retinal degeneration observed in *arrd2* mice shares some similarities with AMD in humans, including late age of onset, fundus hypo-pigmentation and RPE atrophy (16). Furthermore, the critical interval of an AMD susceptibility locus localized to human chromosome 12 includes the human *MDM1* gene (17,18). We have tested the association between *MDM1* and susceptibility to AMD in two cohorts of patients, one a set of families with disease and the other a case–control study. Both of these analyses revealed no significant association between *MDM1* and human AMD. AMD is a multigenic and genetically heterogeneous disease. Lack of association in particular cohorts of patients does not obviate the involvement of the *MDM1* gene product in AMD pathogenesis. It is possible that this gene may not be directly associated with susceptibility to AMD but still may play a major role in the aging retina.

We detected four major transcripts of the *Mdm1* gene including a novel RT. The novel transcript is the predominant transcript in the retina and the highest level of expression of *Mdm1* RT in the retina suggests a critical role for the *Mdm1* RT in retina. Absence of MDM1 protein may affect the retinal function and lead to degeneration. The Arg 399 Stop mutation found in the *Mdm1* gene affects the RT and also the LT but not the ST. The Arg 399 Stop mutation observed in *arrd2* mice is likely to result in nonsense-mediated decay of the transcript, resulting in a null allele or severely depleted truncated protein. The retinal pathology observed in the *arrd2* homozygous mice and lack of pathology in heterozygous mice indicates that the absence of the *Mdm1* gene product may underlie the mechanism leading to retinal degeneration in these mice. Presence of high levels of *Mdm1* ST may compensate for the loss of LT and RT in the testis.

The decrease observed in the levels of expression of photoreceptor-specific genes in *arrd2* mice could be due to the loss of photoreceptor cells rather than specific down regulation of the genes. However, the significant up-regulation observed in stress response gene *Gfap* at 5 months indicates that the biological events leading to degeneration of retina in *arrd2* mice are active by this age. Consistent with these observations, abnormalities were noted in the retinal architecture of arrd2 mice by ultra structural analysis at this age. Finally, alteration of *Casp3* mRNA is consistent with significant photoreceptor loss and indicates activation of apoptosis following initiation of retinal degeneration in *arrd2* mice.

The biological function of the *MDM1* gene is not known. Double minutes are chromosome-associated paired acentromeric extrachromosomal bodies that represent amplified sequences. Double minutes have been described in a variety of tumor cells and transformed cell lines. From the sequences that are amplified and over-expressed in a spontaneously transformed mouse 3T3 cell line, four double minute genes *Mdm1*, *Mdm2*, *Mdm3* and *Mdm4* (or *MdmX*) have been described. *Mdm1*, *Mdm2* and *Mdm3* are located on mouse chromosome 10, whereas *Mdm4* is localized to mouse chromosome 1. Detailed studies were carried out on both *Mdm2* and *MdmX* genes, whereas very limited information is available on the *Mdm1* and *Mdm3* genes. *Mdm2* and *Mdm4* (*MdmX*) negatively regulate the function of P53 in a synergistic manner (19,20). MDM2 is an ubiquitin ligase that catalyses ubiquitination of p53 and itself (21,22). MDM4 inhibits P53 by binding and masking the transcriptional activation domain. It has been demonstrated that MDM2 and MDM4 are required for proper development of the central nervous system. Loss of MDM2 and MDM4 results in a P53 dependent apoptotic phenotype in the developing CNS. In *arrd2* mice with *Mdm1* nonsense mutation, development of retina was found to be normal. Unlike *Mdm2* and *Mdm4* null mice,

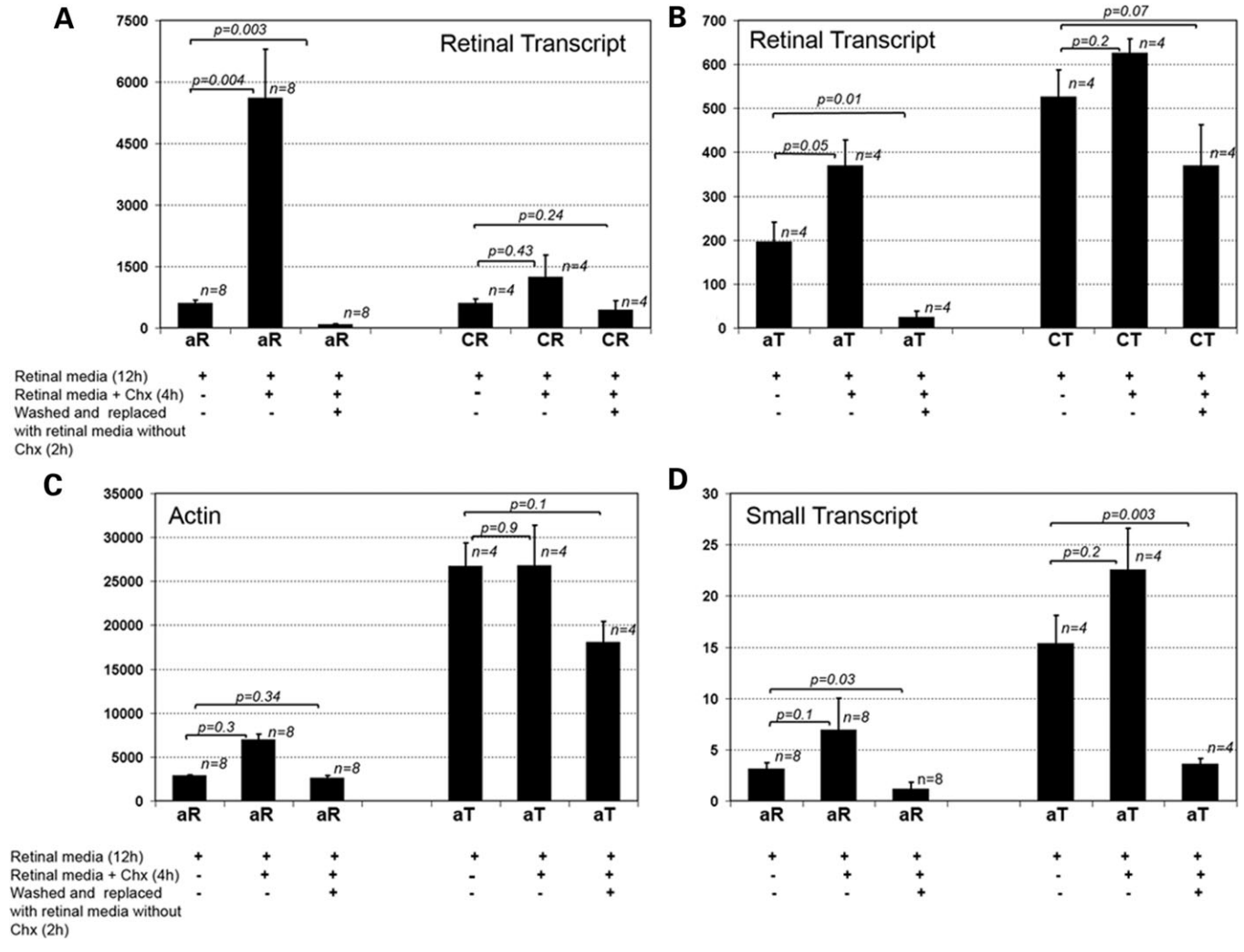

Figure 8. Assay for NMD. Retinal and testis explants from *arrd2* mice and C57BL/6J mice were cultured for 12 h and followed by treatment with 100 ug/ml cycloheximide (Chx) for 4 h. Duplicate samples washed off cycloheximide and incubated in the media for another 2 h. Total RNA was extracted from all the samples converted to cDNA and the message level of the *Mdm1* transcripts which are affected and not affected by the mutation are tested by qRT–PCR. C57BL/6J samples and *β-Actin* transcripts served as controls. The scale on *Y*-axis is fold over *Hgprt* expression. (**A**) Expression of *Mdm1* RT in *arrd2* retina (aR) and C57BL/6J retina (CR). (**B**) Expression of *Mdm1* RT in *arrd2* testis (aT) and C57BL/6J testis (CT). (**C**) Expression of *Actin beta* in *arrd2* retina (aR) and *arrd2* testis (aT). (**D**) Expression of *Mdm1* ST in *arrd2* retina (aR) and *arrd2* testis (aT).

apoptosis in *arrd2* mice appears to be activated much later and subsequent to initiation of photoreceptor loss. Furthermore, no sequence homology was observed between the *Mdm1* and other *Mdms*. Therefore, although the sequence of *Mdm1* is amplified in transformed 3T3 cells, the biological role of this gene may be different from other members of the double minute gene family. Neither the RT nor other transcripts of *Mdm1* showed significant homology with any known sequences. However, presence of a coiled coil domain and reported localization of the *Mdm1* protein to the nucleus suggest a role for MDM1 in transcriptional machinery like MDM2 (13). Additional studies are needed to determine the function of this gene.

Although the expression of *Mdm1* was detected from very early stages of eye development, the onset of retinal degeneration phenotype in *arrd2* mice was observed after 8 months of age. Expression of stress response genes and retinal ultrastructure analysis revealed significant changes in the retina of *arrd2* mice as early as 5 months. Expression of *Mdm1* was found to be increased with age and sustained high levels of expression were maintained at older age in the retina of control mice suggesting the presence of this protein is required in aging retina. The late-onset retinal degeneration observed in these mice is either due to that requirement of high level of MDM1 with age or to a mechanism yet to be determined. Null mutations in other genes expressed at early stages of development leading to late-onset phenotypes have been reported previously (23–25). High levels of *Mdm1* expression are also observed in testis which includes high level of ST which is not affected by the non-sense mutation that might compensate to some extent the loss of LTs. Higher level of ST or low activity of the residual truncated transcript at early ages and/or cumulative effect of the absence of the *Mdm1* gene may underlie the late onset retinal degeneration phenotype in these mice. Evaluation of the functional role of this gene and the mechanism underlying late-onset retinal

degeneration in these mice may reveal the critical biological pathways that operate in maintaining the normal function of aging retinal tissue.

MATERIALS AND METHODS

Animals

The mice in this study were bred and maintained in standard 12 h dark and 12 h light cycle and standardized conditions in the Research Animal Facilities at the Jackson Laboratory, Bar harbor, ME, and University of Michigan, Ann Arbor, MI. They were maintained on NIH 31.6% fat chow and acidified water, with a 14 h light/10 h dark cycle in conventional facilities that were monitored regularly to maintain a pathogen-free environment. All experiments were approved by the Institutional Animal Care and Use Committee and conducted in accordance with the ARVO Statement for the Use of Animals in Ophthalmic and Vision Research.

Clinical retinal evaluation

One hundred and twenty-eight mice used in clinical characterization studies had pupils dilated with 1% atropine ophthalmic eye drops and were evaluated by indirect ophthalmoscopy with a 78 diopter lens. Fundus photographs were taken with a Kowa Genesis small animal fundus camera (Torrance, CA, USA) (26).

Electroretinography

After at least 6 h of dark adaptation, mice were anesthetized with an intraperitoneal injection of normal saline solution containing ketamine (15 mg/gm) and xylazine (7 mg/gm body wt). ERGs were recorded as described earlier (27). Dark-adapted responses were recorded to short-wavelength ($\lambda_{max} = 470$ nm; Wratten 47A filter) flashes of light over a 4.0-log unit range of intensities (0.3 log unit steps) up to the maximum allowable by the photic stimulator. Light-adapted responses were obtained with white flashes (0.3 steps) on the rod-saturating background after 10 min of exposure to the background light to allow complete light adaptation. Signals were sampled every 0.8 ms over a response window of 200 ms. The actual flash intensities used to obtain the representative ERG waves for dark-adapted responses were 0.6 and 2.1 log cd s/m^2 and for light-adapted responses were 0.9 and 1.9 log cd s/m^2, respectively. The ERG response obtained from same mouse at different light intensities and ages is presented in Fig. 1B.

Light and transmission electron microscopy

Both eyes from *arrd2* mutant mice and age-matched C57BL/6J mice were enucleated and eyecups were prepared for light and electron microscopic examination as described previously (27). Two to six eyes were used for each age group. For each sample, 0.5 μm thin sections were stained with toluidine blue for light microscopy followed by ultrathin section preparation for TEM examination.

Gene mapping and sequencing

arrd2 mice were mated with B6 mice and the F1 mice, which exhibit no retinal abnormalities, were intercrossed to produce F2 mice. Tail DNA was isolated as previously reported (28). DNAs of 73 F2 offspring were genotyped using microsatellite markers to develop a structure map of the region. Initially, a genome scan of microsatellite (Mit) DNA markers was carried out on pooled DNA samples (29). After detection of linkage on chromosome 10, individual DNA samples were analyzed with microsatellite markers *D10Mit96, D10Mit78, D10Mit70, D10Mit162, D10Mit135, D10Mit233, D10Mit179, D10Mit164, D10Mit267, D10Mit237, D10Mit297*.

The candidate genes localized to the critical interval between markers *D10Mit179* and *D10Mit267* were identified by scanning the mouse genomic sequence available through NCBI. A total of 35 genes including putative genes have been localized to this interval and 9 of them were reported to be expressed in the retina. We selected these 9 genes for mutation analysis of *arrd2* mice. PCR primers to amplify coding regions were designed using the mouse genomic sequence encompassing the candidate genes. PCR products were purified from agarose gels using a Qiagen kit (Qiagen Inc. Valencia, CA, USA). Sequencing reactions were carried out with automated fluorescence tag sequencing.

RNA isolation and real-time quantitative RT–PCR

To evaluate the transcripts of the *Mdm1* gene and their expression by real-time qRT–PCR, RNA was isolated from different tissues of C57BL/6J mice. Mice were dark-adapted overnight and liver, lungs, brain, ciliary body and iris (eye anterior), posterior segment of the eye (containing RPE, choroid and sclera), retina, lens, cornea, heart, spleen, kidney, skeletal muscle, skin, testis and uterus were collected in TRIzol reagent (Invitrogen, Carlsbad, CA, USA) at the end of the dark cycle. RNA was isolated from these tissues following the manufacturer's protocol. All RNA samples were purified and single strand cDNA was prepared for qRT–PCR.

To study the age-related expression of *Mdm1* in retina, cDNA was prepared from C57BL/6J retina of 20, 35, 50, 180, 300, 420, 500 and 600 days old mice. Similarly, for a comparative study of retinal cell-specific marker gene expression, cDNA was prepared from the retinal RNA of 5, 12 and 18 months old *arrd2* and C57BL/6J mice. Primer pairs to amplify specific transcripts were designed for qRT–PCR (Fig. 4A, Supplementary Table 1). The levels of expression of four genes *Gapdh*, *Hgprt, Actin-β* and *RpL19* were used as controls to normalize the *Mdm1* gene expression and the data were analyzed using previously published protocols (14,30,31). Mean (± SEM) relative expression values calculated from at least three independent samples are presented.

In situ hybridization

A cDNA fragment (620 bp) that specifically recognizes the *Mdm1* LT and RT was amplified from C57BL/6J mice retinal cDNA using primers located in exon 7 (forward) and exon 10 (reverse) and tagged to T7 and T3 promoters,

respectively (Fig. 4A). The sequence of primers will be available from the authors upon request. The *Mdm1* ribo-probes (sense and antisense) were generated by labeling the amplified cDNA fragment using a DIG-RNA labeling kit (Boehringer Mannheim GMBH, Mannheim, Germany). *In situ* hybridizations were performed following previously published protocols (32,33).

Northern blot analysis

Northern blots were generated using 5–7 μg of purified total RNA isolated from kidney, brain, retina and testis of C57BL/6J and *arrd2* mice. *Mdm1* cDNA probe was generated from the same region of the gene that is used for generating the *in situ* hybridization probe. Probe for human *β-ACTIN* gene which recognizes its mouse ortholog was obtained from Clontech. Hybridization was carried out using Express Hyb (Clontech) following previously published protocols (14).

Assay for nonsense-mediated decay

Retinal and testis explants of C57BL/6J and *arrd2* mice were cultured in retinal medium as described by Hatakeyama and Kageyama (34) on millicell cell culture membrane (Millipore, Bedford, MA, USA) for 12 h at 37°C with a 5% atmospheric CO_2 concentration (34). After 12 h, the media was replaced with fresh retinal media in one set of samples which served as controls. The media of the second set of samples was replaced with fresh media containing 100 μg/ml of cycloheximide and incubated for 4 more hours. After 4 h incubation, tissues were harvested from the control sample and one set of the cycloheximide treated samples. The second set of cycloheximide treated replica samples were washed with RNAse free phosphate buffered saline to remove the cycloheximide and incubated for an additional 2 h with fresh retinal medium. Testis tissues from both C57BL/6J and *arrd2* mice were also treated with cycloheximide in a similar manner. Total RNA was isolated from each sample, converted to first-strand cDNA and used for qRT–PCR. Quantitative expression of the *Mdm1* transcripts was determined by qRT–PCR. Expression of the *β-Actin* gene was measured as an internal control for NMD in *arrd2* mice retina and testis samples. C57BL/6J samples served as independent controls for the *Mdm1* nonsense-mediated decay in *arrd2* mice.

Association of *Mdm1* with AMD susceptibility

A cohort of patients from the Family Age-Related Maculopathy Study (FARMS) was examined for evidence of association between *MDM1* and AMD. Subjects were recruited through the Retina Clinic at the University of Wisconsin, Madison and evaluated as previously described (17). The standardized clinical evaluation did not include fluorescein angiography, preventing direct comparison with the angiographic features identified in the current mouse model. Families were identified through severely affected index cases; in all, 293 individuals from 34 families were included in the current study. The human *MDM1* gene was identified by orthology to mouse chromosome 10 and the gene LD structure was analyzed in the HapMap data (CEU population: Centre d'Etude du Polymorphisme Humain) using Haploview (35). We identified two LD blocks in this gene (see Supplementary Material). Three SNPs were chosen to cover the LD blocks, with two SNPs spaced across the larger block. Two of the chosen SNPs code for missense variants. Combining the data on these three SNPs effectively captures most of the common variants within *MDM1* (HapMap pairwise Tagger, $r^2 \geq 0.8$, MAF ≥ 0.2) (36).

Genotyping was conducted as part of a custom GoldenGate Illumina panel. One sample was excluded from the analysis due to a call rate of less than 90% for the entire panel. No inconsistencies in genotyping were detected using MARKER-INFO (S.A.G.E. v5.3) (http://genepi.cwru.edu/) and comparison of 28 replicates. Each SNP was tested for association with a 15 step AMD phenotype severity scale based on standardized grading of stereoscopic 30° color fundus photographs, using a variance component family-based model incorporating both sibling and family effects in ASSOC (S.A.G.E.). SNPs were individually tested under additive, dominant and recessive inheritance models.

As a virtual replication, the database of Genotype and Phenotype (dbGaP) (37) was queried to identify any *MDM1* variants analyzed in a genomewide association analysis conducted by the National Eye Institute Age Related Eye Disease Study (AREDS) (38). The AREDS study examined a Caucasian cohort of approximately 400 severely affected AMD patients and 200 controls using 100 K Affymetrix and Illumina panels, and conducted single marker tests for association with AMD status.

SUPPLEMENTARY MATERIAL

Supplementary Material is available at *HMG* Online.

FUNDING

This study was supported by the grants from the National Institutes of Health grants EY13198, U10EY06594, EY015286, EY13438, EY10605, EY015810, NIH T32-EY07157, T32 GM007250, EY07758, RR01183, Research to Prevent Blindness, Inc., New York, NY (R.A.) and EY07758 (B.C.). Foundation Fighting Blindness (R.A., J.R.H., B.C.), Retina Research foundation. Institutional shared services are supported by National Cancer Institute, Cancer Center grant CA34196. The results of this paper were obtained by using the software package S.A.G.E., which is supported by a US Public Health Service Resource Grant (RR03655) from the National Center for Research Resources. This research was supported by the Gene Expression and Genotyping Facility of the Comprehensive Cancer Center of Case Western Reserve University and University Hospitals of Cleveland (P30CA43703).

ACKNOWLEDGEMENTS

The authors thank Austra Liepa for maintenance of the mice, and technical assistance, and Mitchell Gillett for tissue preparation for morphological analysis.

Conflict of Interest statement. None declared.

REFERENCES

1. Chang, B., Hawes, N.L., Hurd, R.E., Davisson, M.T., Nusinowitz, S. and Heckenlively, J.R. (2002) Retinal degeneration mutants in the mouse. *Vision Res.*, **42**, 517–525.
2. Marmorstein, A.D. and Marmorstein, L.Y. (2007) The challenge of modeling macular degeneration in mice. *Trends Genet.*, **23**, 225–231.
3. Elizabeth Rakoczy, P., Yu, M.J., Nusinowitz, S., Chang, B. and Heckenlively, J.R. (2006) Mouse models of age-related macular degeneration. *Exp. Eye Res.*, **82**, 741–752.
4. Hamdi, H.K. and Kenney, C. (2003) Age-related macular degeneration: a new viewpoint. *Front. Biosci.*, **8**, 305–314.
5. Fine, S.L., Berger, J.W., Maguire, M.G. and Ho, A.C. (2000) Age-related macular degeneration. *N. Eng. J. Med.*, **342**, 483–492.
6. Hageman, G.S., Luthert, P.J., Victor Chong, N.H., Johnson, L.V., Anderson, D.H. and Mullins, R.F. (2001) An integrated hypothesis that considers drusen as biomarkers of immune-mediated processes at the RPE-Bruch's membrane interface in aging and age-related macular degeneration. *Prog. Retin. Eye Res.*, **20**, 705–732.
7. Lutty, G., Grunwald, J., Majji, A.B., Uyama, M. and Yoneya, S. (1999) Changes in choriocapillaris and retinal pigment epithelium in age-related macular degeneration. *Mol. Vis.*, **5**, 35.
8. Klein, R.J., Zeiss, C., Chew, E.Y., Tsai, J.Y., Sackler, R.S., Haynes, C., Henning, A.K., SanGiovanni, J.P., Mane, S.M., Mayne, S.T. *et al.* (2005) Complement factor H polymorphism in age-related macular degeneration. *Science*, **308**, 385–389.
9. Gold, B., Merriam, J.E., Zernant, J., Hancox, L.S., Taiber, A.J., Gehrs, K., Cramer, K., Neel, J., Bergeron, J., Barile, G.R. *et al.* (2006) Variation in factor B (BF) and complement component 2 (C2) genes is associated with age-related macular degeneration. *Nat. Genet.*, **38**, 458–462.
10. Vasireddy, V., Uchida, Y., Salem, N., Kim, S.Y., Mandal, M.N., Reddy, G.B., Bodepudi, R., Alderson, N.L., Brown, J.C., Hama, H. *et al.* (2007) Loss of functional ELOVL4 depletes very long-chain fatty acids (>=C28) and the unique {omega}-O-acylceramides in skin leading to neonatal death. *Hum. Mol. Genet.*, **16**, 471–482.
11. Kanda, A., Chen, W., Othman, M., Branham, K.E., Brooks, M., Khanna, R., He, S., Lyons, R., Abecasis, G.R. and Swaroop, A. (2007) A variant of mitochondrial protein LOC387715/ARMS2, not HTRA1, is strongly associated with age-related macular degeneration. *Proc. Natl Acad. Sci. USA*, **104**, 16227–16232.
12. Cahilly-Snyder, L., Yang-Feng, T., Francke, U. and George, D.L. (1987) Molecular analysis and chromosomal mapping of amplified genes isolated from a transformed mouse 3T3 cell line. *Somat. Cell Mol. Genet.*, **13**, 235–244.
13. Snyder, L.C., Trusko, S.P., Freeman, N., Eshleman, J.R., Fakharzadeh, S.S. and George, D.L. (1988) A gene amplified in a transformed mouse cell line undergoes complex transcriptional processing and encodes a nuclear protein. *J. Biol. Chem.*, **263**, 17150–17158.
14. Mandal, M.N., Ambasudhan, R., Wong, P.W., Gage, P.J., Sieving, P.A. and Ayyagari, R. (2004) Characterization of mouse orthologue of ELOVL4: genomic organization and spatial and temporal expression. *Genomics*, **83**, 626–635.
15. Chader, G.J. (2002) Animal models in research on retinal degenerations: past progress and future hope. *Vision Res.*, **42**, 393–399.
16. Klein, R. (2007) Overview of progress in the epidemiology of age-related macular degeneration. *Ophthalmic Epidemiol.*, **14**, 184–187.
17. Iyengar, S.K., Song, D., Klein, B.E., Klein, R., Schick, J.H., Humphrey, J., Millard, C., Liptak, R., Russo, K., Jun, G. *et al.* (2004) Dissection of genomewide-scan data in extended families reveals a major locus and oligogenic susceptibility for age-related macular degeneration. *Am. J. Hum. Genet.*, **74**, 20–39.
18. Fisher, S.A., Abecasis, G.R., Yashar, B.M., Zareparsi, S., Swaroop, A., Iyengar, S.K., Klein, B.E., Klein, R., Lee, K.E., Majewski, J. *et al.* (2005) Meta-analysis of genome scans of age-related macular degeneration. *Hum. Mol. Genet.*, **14**, 2257–2264.
19. Xiong, S., Van Pelt, C.S., Elizondo-Fraire, A.C., Liu, G. and Lozano, G. (2006) Synergistic roles of Mdm2 and Mdm4 for p53 inhibition in central nervous system development. *Proc. Natl Acad. Sci. USA*, **103**, 3226–3231.
20. Badciong, J.C. and Haas, A.L. (2002) MdmX is a RING finger ubiquitin ligase capable of synergistically enhancing Mdm2 ubiquitination. *J. Biol. Chem.*, **277**, 49668–49675.
21. Coutts, A.S. and La Thangue, N.B. (2007) Mdm2 widens its repertoire. *Cell Cycle*, **6**, 827–829.
22. Lukashchuk, N. and Vousden, K.H. (2007) Ubiquitination and degradation of mutant p53. *Mol. Cell. Biol.*, **27**, 8284–8295.
23. Takahashi, Y., Miyajima, H., Shirabe, S., Nagataki, S., Suenaga, A. and Gitlin, J.D. (1996) Characterization of a nonsense mutation in the ceruloplasmin gene resulting in diabetes and neurodegenerative disease. *Hum. Mol. Genet.*, **5**, 81–84.
24. Das, A.K., Lu, J.Y. and Hofmann, S.L. (2001) Biochemical analysis of mutations in palmitoyl-protein thioesterase causing infantile and late-onset forms of neuronal ceroid lipofuscinosis. *Hum. Mol. Genet.*, **10**, 1431–1439.
25. Souied, E.H., Ducroq, D., Rozet, J.M., Gerber, S., Perrault, I., Sterkers, M., Benhamou, N., Munnich, A., Coscas, G., Soubrane, G. *et al.* (1999) A novel ABCR nonsense mutation responsible for late-onset fundus flavimaculatus. *Invest. Ophthalmol. Vis. Sci.*, **40**, 2740–2744.
26. Hawes, N.L., Smith, R.S., Chang, B., Davisson, M., Heckenlively, J.R. and John, S.W. (1999) Mouse fundus photography and angiography: a catalogue of normal and mutant phenotypes. *Mol. Vis.*, **5**, 22.
27. Hawes, N.L., Chang, B., Hageman, G.S., Nusinowitz, S., Nishina, P.M., Schneider, B.S., Smith, R.S., Roderick, T.H., Davisson, M.T. and Heckenlively, J.R. (2000) Retinal degeneration 6 (rd6): a new mouse model for human retinitis punctata albescens. *Invest. Ophthalmol. Vis. Sci.*, **41**, 3149–3157.
28. Buffone, G.J. and Darlington, G.J. (1985) Isolation of DNA from biological specimens without extraction with phenol. *Clin. Chem.*, **31**, 164–165.
29. Taylor, B.A., Navin, A. and Phillips, S.J. (1994) PCR-amplification of simple sequence repeat variants from pooled DNA samples for rapidly mapping new mutations of the mouse. *Genomics*, **21**, 626–632.
30. Mandal, M.N. and Ayyagari, R. (2006) Complement factor H: spatial and temporal expression and localization in the eye. *Invest. Ophthalmol. Vis. Sci.*, **47**, 4091–4097.
31. Mandal, M.N., Vasireddy, V., Reddy, G.B., Wang, X., Moroi, S.E., Pattnaik, B.R., Hughes, B.A., Heckenlively, J.R., Hitchcock, P.F., Jablonski, M.M. *et al.* (2006) CTRP5 is a membrane-associated and secretory protein in the RPE and ciliary body and the S163R mutation of CTRP5 impairs its secretion. *Invest. Ophthalmol. Vis. Sci.*, **47**, 5505–5513.
32. Levine, E.M., Passini, M., Hitchcock, P.F., Glasgow, E. and Schechter, N. (1997) Vsx-1 and Vsx-2: two Chx10-like homeobox genes expressed in overlapping domains in the adult goldfish retina. *J. Comp. Neurol.*, **387**, 439–448.
33. Hitchcock, P.F., Otteson, D.C. and Cirenza, P.F. (2001) Expression of the insulin receptor in the retina of the goldfish. *Invest. Ophthalmol. Vis. Sci.*, 2125–2129.
34. Hatakeyama, J. and Kageyama, R. (2002) Retrovirus-mediated gene transfer to retinal explants. *Methods*, **28**, 387–395.
35. Barrett, J.C., Fry, B., Maller, J. and Daly, M.J. (2005) Haploview: analysis and visualization of LD and haplotype maps. *Bioinformatics*, **21**, 263–265.
36. de Bakker, P.I., Yelensky, R., Pe'er, I., Gabriel, S.B., Daly, M.J. and Altshuler, D. (2005) Efficiency and power in genetic association studies. *Nat. Genet.*, **37**, 1217–1223.
37. Mailman, M.D., Feolo, M., Jin, Y., Kimura, M., Tryka, K., Bagoutdinov, R., Hao, L., Kiang, A., Paschall, J., Phan, L. *et al.* (2007) The NCBI dbGaP database of genotypes and phenotypes. *Nat. Genet.*, **39**, 1181–1186.
38. Age-Related Eye Disease Study Research Group. (2000) Risk factors associated with age-related macular degeneration. A case-control study in the age-related eye disease study: Age-Related Eye Disease Study Report Number 3. *Ophthalmology*, **107**, 2224–2232.